International Journal of Heat and Technology
Vol. 40, No. 1, February, 2022, pp. 311-318
Journal homepage: http://iieta.org/journals/ijht

Numerical Analysis and Optimization of Heat Dissipation of Mechanical Automation Equipment Based on Thermal Model

Miaomiao Zhang

School of Intelligent Manufacturing, Zibo Vocational College, Zibo 255300, China

Corresponding Author Email: zbvc11465@zb.shandong.cn

https://doi.org/10.18280/ijht.400137

Received: 21 October 2021
Accepted: 6 January 2022

Keywords:
thermal model, mechanical automation equipment, heat dissipation, numerical simulation

ABSTRACT

If the internal heat of mechanical automation equipment exceeds or does not reach the thermal equilibrium temperature range, it will adversely affect the operational reliability, environmental protection and production efficiency of the equipment. To tackle the problem, there has been some research on the internal heat dissipation of mechanical automation equipment, but mostly of the existing studies have simply aimed to change the parameters of the cooling system, and little has been done on the loading process and implementation details of the thermal model. Therefore, this paper provides numerical analysis and optimization of the space heat dissipation of mechanical automation equipment based on a thermal model. First, the heat dissipation mechanism of mechanical automation equipment was elaborated in detail, and the structure of the cooling system for mechanical automation equipment was given. Then, a spatial thermal model of mechanical automation equipment was established, and the heat dissipation design process of mechanical automation equipment was given. After that, the differences between the natural convection heat dissipation in large space and that in confined space inside mechanical automation equipment were explored. The experimental results verified the effectiveness of the numerical simulation model proposed in this paper.

1. INTRODUCTION

A piece of mechanical automation equipment is both a heat source and a source of heat dissipation. If the internal heat of the mechanical automation equipment exceeds or does not reach the thermal equilibrium temperature range, it will adversely affect the operational reliability, environmental protection and production efficiency of the equipment [1-6]. Theories and practices have shown that, only when the heat generation and dissipation of the mechanical automation equipment reach the best equilibrium, can the mechanical automation equipment be in an efficient, energy-saving and environmentally friendly operation state [7-11]. In the manufacturing process of mechanical automation equipment, the inspection on all kinds of components is very strict, so that they will be able to withstand the test of harsh environments in practical applications [12-15]. Fans are an indispensable and important part of the cooling system of mechanical automation equipment. The noise of the main equipment, the economy of fuel and the cooling effect of the cooling system are all affected by the choice of fans [16-18]. Besides, there are also various other influencing factors that can affect the thermal environment inside the mechanical automation equipment. It is important to analyze all these factors, and explore effective measures to optimize the cooling conditions of the equipment, as this will provide references for the use of related equipment or engineering design.

Wang et al. [19] studied a high-performance air cooling system with uniform heating plate temperature distribution and developed a fin and multi-flow air duct system, where there are rows of small inclined protrusions on the surfaces of the fins to improve the cooling performance. The multi-flow air duct system can bypass the fresh low-temperature air around the lower plate to promote the uniform temperature distribution of the plate. Satake et al. [20] studied the structure of the real-time heat dissipation model of electronic equipment according to the law of energy conservation, Laplace transform and other methods and determined that the model structure was an 11^{th}-order transfer function. It built an experimental device to collect the heat dissipation and power consumption data of typical electronic equipment for parameter identification and model verification, and identified the unknown parameters in the real-time heat dissipation model. Through order reduction analysis, the third-order transfer function was selected as the heat dissipation model. This model not only describes the dynamicness and randomness of the heat dissipation of electronic equipment, but it is also of great significance to the calculation of the instantaneous cooling demand and energy saving. To quantitatively analyze the heat dissipation of high-power equipment, Li et al. [21] used the software Icepak to analyze and compare the effects of fans on heat dissipation. It established two models, one with fans and the other without them, and combined the mesh around the radiators with structured and unstructured meshes based on the advantages of Icepak. Karami et al. [22] conducted laboratory experiments at the real scale to fully describe the heat transfer between the fluid and the device. In some specific area of interest, to estimate the convective heat transfer coefficient, it directly measured the temperature distribution from the sub-layers to the wall, performed a large eddy simulation coupled with a thermal solver, and compared the results with experimental

data, enabling cross-validation between simulation and experiment. Kuntysh et al. [23] proposed a new boiling critical heat flow model for porous coatings based on the analysis of liquid film stability analysis, and described the parameter effects of porous coatings on CHF. The analytical model was in good agreement with the experimental results.

The working environment of mechanical automation equipment is relatively harsh. Before the use environment is determined, it is difficult to understand its specific temperature characteristics. Foreign research has mainly focused on improving the heat dissipation performance within the internal space and paid less attention to the overall evaluation of the heat dissipation performance of the equipment during the design process. The research on heat dissipation in the internal space of mechanical automation equipment is also limited to simply changing the parameters of the cooling system, and little has been done on the loading process and implementation details of the thermal model. This paper focuses on analyzing the optimization conditions for the application of the cooling system for mechanical automation equipment, and performing numerical analysis and optimization of the space heat dissipation of mechanical automation equipment based on a thermal model. The whole paper is organized as follows: 1) the heat dissipation mechanism of the mechanical automation equipment is elaborated, and the structure of the cooling system of the mechanical automation equipment is given; 2) the spatial thermal model of the mechanical automation equipment is constructed; 3) the heat dissipation design process of the mechanical automation equipment is given; 4) the differences between the natural convection heat dissipation in large space and that in confined space inside mechanical automation equipment are explored; 5) the radiator check process for individual components is provided. The experimental results verified the effectiveness of the proposed numerical simulation model.

2. HEAT DISSIPATION MECHANISM IN THE INTERNAL SPACE OF MECHANICAL AUTOMATION EQUIPMENT

A piece of mechanical automation equipment is both a heat source and a source of heat dissipation. The drive system, speed control system and transmission system of any mechanical automation equipment being too cold or too hot ill adversely affect the equipment and even lead to engineering incidents. so a cooling system is required in the mechanical automation equipment to ensure the normal temperature rise inside the equipment and the normal production or operation of the equipment. When the equipment works at the optimal temperature, its working efficiency, energy saving and environmental protection will be improved. Figure 1 simulates the shell structure of a piece of mechanical automation equipment.

The heat dissipation mechanism of mechanical automation equipment is shown in Figure 2. The whole equipment adopts air cooling for heat dissipation. The radiator set consists of an oil radiator for the drive system, an oil radiator for the transmission system torque converter and an intercooler and a water cooling radiator for the speed control system, which dissipate the heat in all kinds of parts and finally make all parts of the mechanical automation equipment work at a suitable temperature. Figure 3 shows the schematic diagram of the cooling system of the mechanical automation equipment.

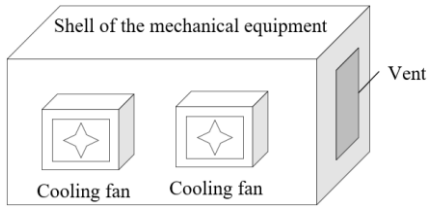

Figure 1. Shell structure of mechanical automation equipment

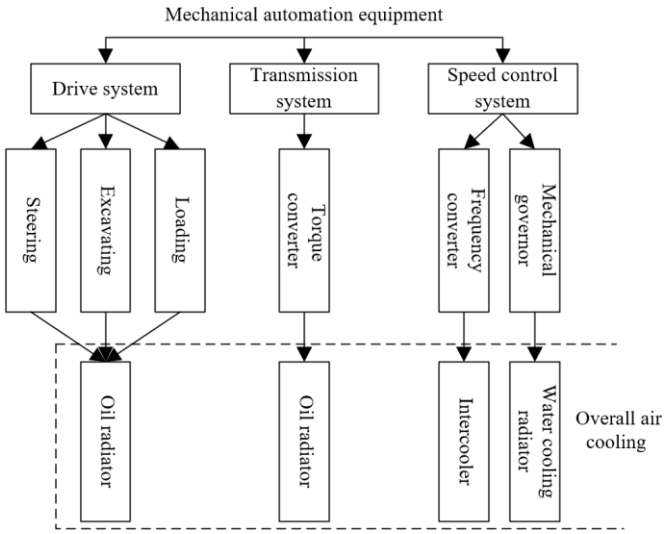

Figure 2. Heat dissipation mechanism of mechanical automation equipment

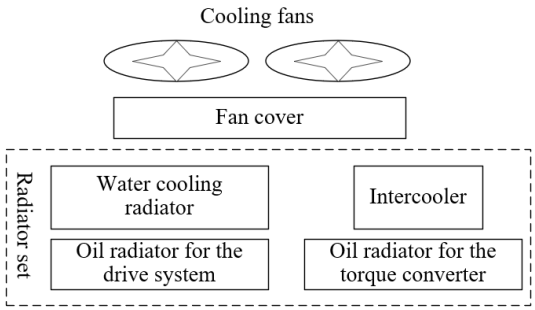

Figure 3. Cooling system of mechanical automation equipment

3. CONSTRUCTION OF THE SPATIAL THERMAL MODEL FOR MECHANICAL AUTOMATION EQUIPMENT

The internal space of a piece of mechanical automation equipment is a typical linear system because all components are linear components. For this linear system, the input is the power consumption of all components, and the state variable is the temperature of each monitoring point in the entire internal space of the equipment. Let the number of power-consuming components be represented by N, and the number of monitoring points in the internal space by M, and $M \geq N$. Then, let the distance between monitoring points i and j be s_{ii}, and the temperature value of monitoring point I be EL_{ij}. Assuming that the internal space temperature vector of the mechanical automation equipment is represented by $a(\tau)=(a_1(\tau), ..., a_M(\tau))^T$, and that the power consumption vector by $o(\tau)$, when $o(\tau)$ is expanded by M-N 0's, the new vector

obtained is represented by $\hat{o}(\tau)=(o_1(\tau), ..., o_M(\tau),0, ..., 0)^T$. And then, the thermal system model for the internal space of mechanical automation equipment can be constructed as follows:

$$EL_i\dot{a}_i(\tau)=-\sum_{j=1}^{M}\frac{1}{s_{ij}}\left(a_i(\tau)-a_j(\tau)\right)+\hat{o}_i(\tau) \quad i=1,2,...,M \tag{1}$$

Let $QE=(QE_{ij})_{M\times M}$,$QF=(QF_{ij})_{M\times M}$, and then there is:

$$QE_{ij}=\begin{cases}-\sum_{l=1}^{M}\frac{1}{s_{il}} & if \quad i=j\\ \frac{1}{s_{il}} & if \quad i\neq j\end{cases} \tag{2}$$

$$QF_{ij}=\begin{cases}QF_i & if \quad i=j\\ 0 & if \quad i\neq j\end{cases} \tag{3}$$

Assuming that the diagonal matrix is represented by DJ, Eq. (1) can be further transformed into:

$$DJ\dot{a}(\tau)=QSa(\tau)+\hat{o}(\tau) \tag{4}$$

Based on DJ, its inverse matrix DJ^{-1} can be calculated. Multiply both sides of the equation shown in Eq. (4) by DJ^{-1}, and then there is:

$$\dot{a}(\tau)=DJ^{-1}QEa(\tau)+DJ^{-1}\tilde{o}(\tau) \tag{5}$$

For DJ^{-1}, when $i>N$, $\hat{o}_i=0$ is only valid to column N on the left side. Therefore, an $M\times N$ matrix H can be constructed to characterize the values of column N on the left side of DJ^{-1}, and let

$$\begin{cases}G=DJ^{-1}QS\\ H=DJ_{LM}^{-1}\end{cases} \tag{6}$$

The input power consumption trajectory of the mechanical automation equipment can be viewed as a series of power consumption vectors. It can be considered that in a small time period $\Delta\tau$, the power consumption vector $o(\tau)$ is fixed, and then there is the temperature vector:

$$a(\Delta\tau)=e^{G\Delta t}a(0)+\left[\int_0^{\Delta\tau}e^{G(\Delta\tau-t)}Hdt\right]\cdot o \tag{7}$$

To reduce the computational load, let the state equation parameter matrices X and Y be expressed as:

$$X=e^{G\Delta\tau},Y=\int_0^{\Delta\tau}e^{G(\Delta\tau-t)}Hdt \tag{8}$$

Combine the equations and there is:

$$a(\Delta\tau)=Xa(0)+Yo \tag{9}$$

Suppose that the input power consumption vector in the time period $[(m-1)\Delta\tau, m\Delta\tau]$ is represented by $o(m-1)$. Since the mechanical automation equipment is a linear time-invariant system, the same X and Y can be used to construct an equation for any small time period $\Delta\tau$:

$$a(m\Delta\tau)=Xa\left((m-1)\Delta\tau\right)+Yo(m-1) \tag{10}$$

Let $a(m\Delta\tau)$ be denoted as $a(m)$. Eq. (11) shows the iterative formula for calculating the internal space temperature vector of the mechanical automation equipment:

$$a(m)=Xa(m-1)+Yo(m-1) \tag{11}$$

For a specific piece of mechanical automation equipment and fixed internal environment, the state equation parameter matrices X and Y only depend on the time period $\Delta\tau$, that is, as long as $\Delta\tau$, X and Y are determined, the constant matrix can be determined. $o(m-1)$ is the input excitation of the linear system of the mechanical automation equipment, that is, the power consumption vector of all components of the equipment in the previous time period. In the internal space temperature vector equation of the mechanical automation equipment shown above, there are only simple matrix addition and multiplication operations. Compared with the thermal model that requires calculus operations, the operation process is much simpler, and the calculation efficiency is much higher. Therefore, it is an ideal thermal simulation model for the internal space of mechanical automation equipment.

4. CALCULATION OF THE HEAT DISSIPATION IN THE SPACE OF THE MECHANICAL AUTOMATION EQUIPMENT

Figure 4 shows the heat dissipation design process of the mechanical automation equipment. Based on the thermal model, the natural convection heat dissipation in the internal space of the mechanical automation equipment can be fully studied, and through the relevant numerical simulation equations, the heat dissipation power of each component in the internal space of the mechanical automation equipment can be calculated.

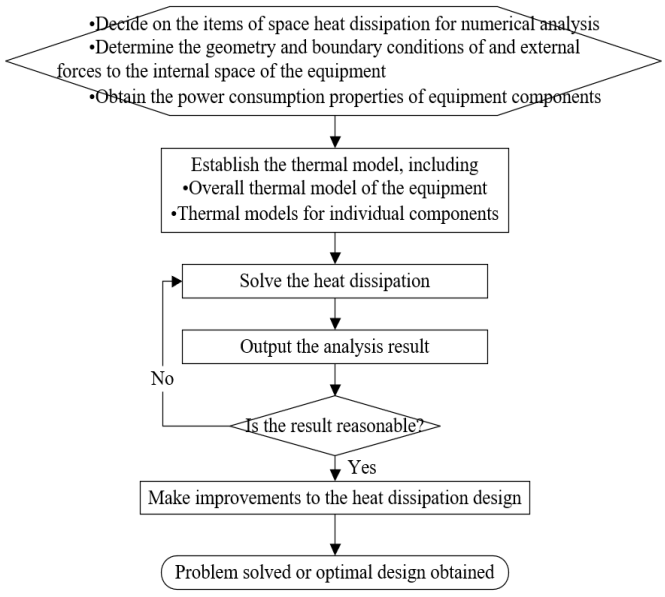

Figure 4. Heat dissipation design process of mechanical automation equipment

This paper previously performed relevant simulation calculation of the parts evenly distributed in the internal space of the mechanical automation equipment, but the calculation amount is rather limited. In practice, the internal space of the mechanical automation equipment is often limited. This paper hopes to explore the differences between the natural convection heat dissipation in large spaces and the natural convection heat dissipation in the confined space inside mechanical automation equipment, and optimize the established thermal model so that it can be applicable to the heat dissipation in the internal spaces of mechanical equipment of different specifications. This will provide some references in the practical application of the model in mechanical automation equipment.

The following section explores the method to calculate the natural convection heat dissipation in the confined space inside the mechanical automation equipment. If radiant heat loss is ignored, the heat dissipation of an individual component can be divided into two parts – the natural convection heat dissipation between the component and the internal environment of the equipment, and the natural convection heat dissipation between the component and other components or the main body of the equipment.

Suppose that the volume change coefficient is represented by γ_p, and for ideal gas, the reciprocal of the absolute temperature can be taken as γ_p. The acceleration of gravity is represented by h, the feature scale by K, the temperature difference by $\Delta\xi$, the convective heat transfer coefficient of the thermal fluid in the mechanical automation equipment by f, the thermal conductivity of the static fluid by l, the heat flow viscosity by λ, and the isobaric specific heat capacity by χ_σ, the thermal diffusion coefficient of heat flow by μ, and the kinematic viscosity of heat flow by η. The convective heat dissipation between the component widely used in the project and other components or the main body of the equipment is expressed as Eq. (12):

$$Nu = \chi\left(Pr, Gr\right)^m \tag{12}$$

where, Nu is the Nusselt number, and there is:

$$Nu = \frac{fK}{l} \tag{13}$$

Pr is used to measure the ratio of heat flow momentum diffusion thickness to heat diffusion thickness, as follows:

$$Pr = \frac{\theta}{\mu} = \frac{\lambda\chi_\sigma}{l} \tag{14}$$

Gr is used to measure the ratio of heat flow buoyancy lift to viscous force, expressed as Eq. (15):

$$Gr = \frac{h\gamma_\eta \Delta\xi K^3}{\eta^3} \tag{15}$$

Figure 5 shows the shares of heat dissipation from mechanical automation equipment based on the air cooling system. The input power of the equipment will directly act on the equipment motor. When the motor converts and outputs the input power into mechanical power, it will consume part of the power for heat dissipation and loss. In addition, the drive and speed control devices will also release some heat.

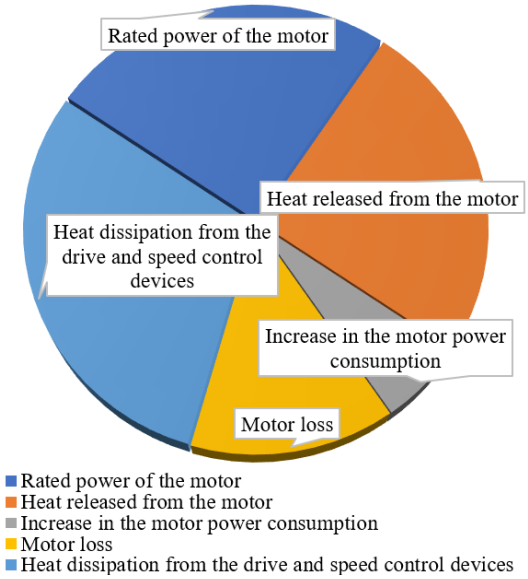

Figure 5. Shares of heat dissipation from mechanical automation equipment

When the internal structure of the equipment is fixed, the heat transfer area and convective heat transfer coefficient of each component can be directly calculated, so the heat transfer in the confined space inside the mechanical automation equipment can also be calculated. Due to the complex heat transfer in the confined space inside the mechanical automation equipment under the actual working environment, the radiant heat transfer is not considered in the calculation of the natural convection heat dissipation between the components and the internal environment of the equipment. Assuming that the number of components is represented by m, Eq. (16) shows the calculation formula of the equivalent area of the components in direct contact with the internal environment of the equipment:

$$X = r \times K \times (m-1) \tag{16}$$

The empirical equation of natural convection heat dissipation between components and the internal environment of the equipment can be calculated through experiments:

Case 1: when the ratio of component spacing to component height is less than 0.3, the space inside the mechanical automation equipment is considered confined, and the feature scale uses the height of the confined space, and there is:

$$Gr = h \cdot \omega \cdot F^3 / \eta^2 \tag{17}$$

Let the dimensionless number UP satisfy:

$$UP = Pr \cdot Gr \le 5 \times 10^6 \tag{18}$$

Nu can be calculated by the following equation:

$$Nu = 1 + 1.5 \times \left(1 - \frac{1650}{UP}\right) + \left[\sqrt[3]{\frac{UP}{6100}} - 1\right] \tag{19}$$

Case 2: when the ratio of component spacing to component height is greater than 0.3, the internal space of the mechanical automation equipment is considered not confined, and the feature scale is set to be $(r+K)/2$, and then there is:

$$Gr = h \cdot \alpha \cdot \omega \cdot \left[\left(r + K \right) / 2 \right]^3 / \eta^2 \tag{20}$$

There are three situations:

$$\text{when } UP < 2 \times 10^4, Nu = 1 \tag{21}$$

$$\text{when } 2 \times 10^4 \le UP < 5 \times 10^6, Nu = 0.6 \cdot \sqrt[4]{UP} \tag{22}$$

$$\text{when } 5 \times 10^6 \le UP < 2 \times 10^{10}, Nu = 0.6 \cdot \sqrt[3]{UP} \tag{23}$$

According to the definition of Nusselt number *Nu*, $f = Nu \times l / F$.

Suppose that the temperature difference between the component and the internal environment of the equipment is denoted as ω. Eq. (21) shows the calculation formula for the heat transfer between the component and the internal environment of the equipment:

$$\omega = f \cdot (m-1) \cdot \omega \cdot r \cdot K \tag{24}$$

For the heat dissipation of a single component, due to the fact that there is a certain temperature difference from the installation position to the top of the component in real practice, the component is treated as a non-isothermal module. The actual heat transfer is rather complex. To simplify it, the following assumptions are made in this paper: 1) the temperature changes only along the height direction of the component; 2) the top of the component is thermally insulated; 3) the material of the component is uniform, with fixed thermophysical properties; 4) the heat flow inside the mechanical automation equipment is an incompressible fluid with fixed thermophysical properties; 5) all thermal contact resistances and thermal spreading resistances are ignored. If the heat dissipation of the component reaches a steady state and the radiant heat transfer is not considered, when the ratio of component spacing to component height is greater than 0.3, it can be considered that the internal space of the mechanical automation equipment is not confined, and the feature scale should be the height of the component *F*. And then, there is the corresponding calculation formula of *Gr*:

$$Gr_{SS} = h \cdot \sigma \left(W_{SS} / \left(2 \cdot F \cdot K \right) \right) \cdot F^4 / \left(l_g \cdot \eta^2 \right) \tag{25}$$

The corresponding *UP* can be calculated according to the following equation:

$$UP_{SS} = Pr_{SS} \cdot Gr_{SS} \tag{26}$$

The corresponding *Nu* can be calculated according to the following equation:

$$Nu_{SS} = 0.55 \cdot UP_{SS} \tag{27}$$

When the ratio of component spacing to component height is less than 0.3, the space inside the mechanical automation equipment is considered confined space, and the feature scale is set at *r*/2, and there are the following three situations:

$$\text{when } UP_{SS} < 10^4, Nu_{SS} = 1 \tag{28}$$

$$\text{when } 10^4 \le UP_{SS} < 10^7, Nu_{SS} = 0.39 \cdot \sqrt[4]{UP_{SS}} \cdot Pr_{SS}^{0.012} \cdot \left(\frac{F}{r/2} \right)^{-0.3} \tag{29}$$

$$\text{when } 10^7 \le UP_{SS} < 10^9, Nu_{SS} = 0.44 \cdot \sqrt[3]{UP_{SS}} \tag{30}$$

The natural convection heat transfer between a single component and the internal environment of the equipment can be calculated according to Eq. (31):

$$W_{SS} = l_{SS} \cdot X_d \cdot \omega^* \cdot n \cdot tanh(n \cdot F) \tag{31}$$

where,

$$n = \sqrt{f_{SS} \cdot v_{SS} \left(l_{SS} \cdot X \right)} \tag{32}$$

The total heat dissipation of all components and the internal environment of the equipment is:

$$W_{ALL} = W + m \cdot W_{SS} \tag{33}$$

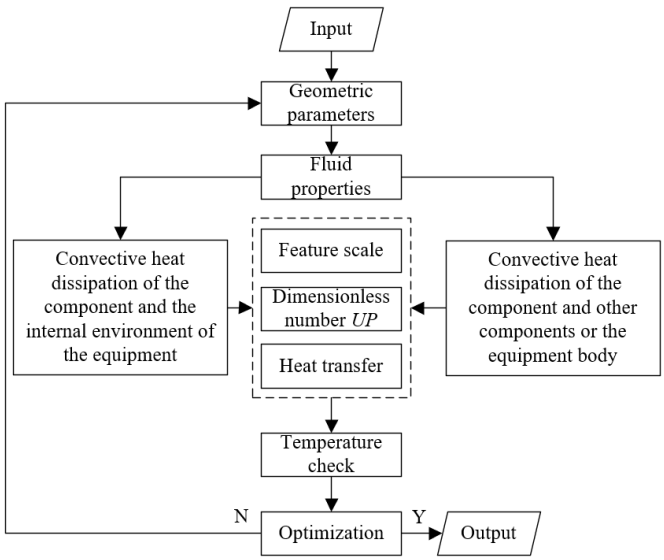

Figure 6. Flow chart of radiator checking for a single component

According to the characteristics of the cooling system of the mechanical automation equipment, the radiator checking process for a single component is shown in Figure 6. In the checking process, analyze the two types of natural convection heat dissipation according to the geometric parameters of the radiators, including feature scale, *UP*, heat transfer and so on. Then check the working temperature of each component so as to complete the checking of the whole equipment.

5. EXPERIMENTAL RESULTS AND ANALYSIS

Figure 7 shows the effects of component spacing on the average temperature of the equipment space. It can be seen that, with the spacing between components gradually increasing, the average temperature of the equipment space also showed a steady upward trend. When the component spacing was 22.6mm, the average temperature of the equipment space was

414.2K. In the case that the internal space of mechanical automation equipment was confined, the average temperature of the equipment space was 414.8K under the same simulation conditions. And when the component spacing reached the limit - the entire width of the component, the temperature reached the average temperature of the equipment space.

In the simulation experiment, the component spacing was set at 2, 3, 4, 5, 6, 7, 8, 9, 10, 11, 12, 13 and 14mm. The average temperatures of the equipment space under different component spacing were calculated, with the results shown in Table 1. For the above simulation examples, to explore the differences between the natural convection heat dissipation in large space and that in the confined space inside the mechanical automation equipment, a series of changes and calculations are required. Below is the derivation and calculation of the differences between the two, with the results shown in Table 2.

Compared with the thermal conductivity and convective heat transfer coefficients of the air, the thermal conductivity coefficient of a component is larger. Therefore, the difference between the average temperature of the equipment space and the temperature of components is not large. Assuming that the average temperature of the equipment space is the same as the temperature of components, it can be said that the temperature difference between the radiators and the environment is approximately equal to the temperature difference between the equipment space and the environment. The relevant data are shown in Table 3.

Table 4 shows the measured average temperatures at the temperature monitoring positions under different models. Figure 8 compares the computational accuracy of different models. It can be seen from the above experimental results that the calculation results of the standard *k-ε* model, the *RNG k-ε* model and the proposed model were all higher than the experimental values. It can be further found that the results of the proposed model were closer to the experimental values than those of the standard *k-ε* model and the *RNG k-ε* model. The calculation results of the standard k-ε model are quite different from experimental values, while those of the *RNG k-ε* model are closer to the experimental values. From the accuracy of the calculation results shown in Figure 8, the effect of the proposed model is the best, showing its effectiveness.

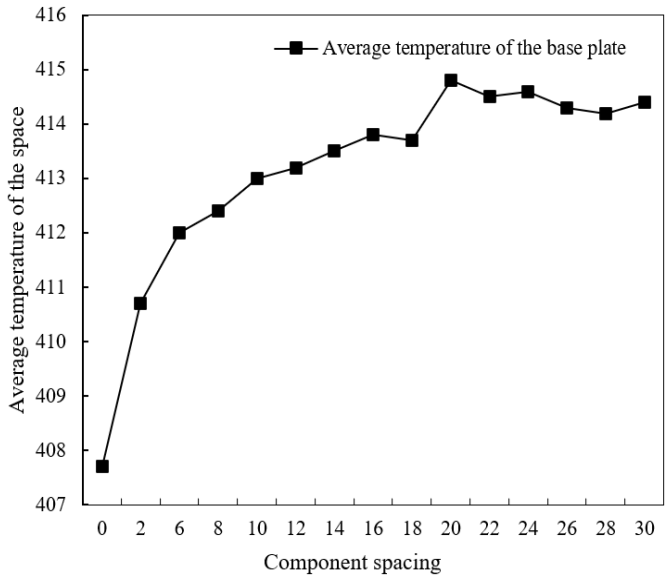

Figure 7. Effects of component spacing on the average temperature of the equipment space

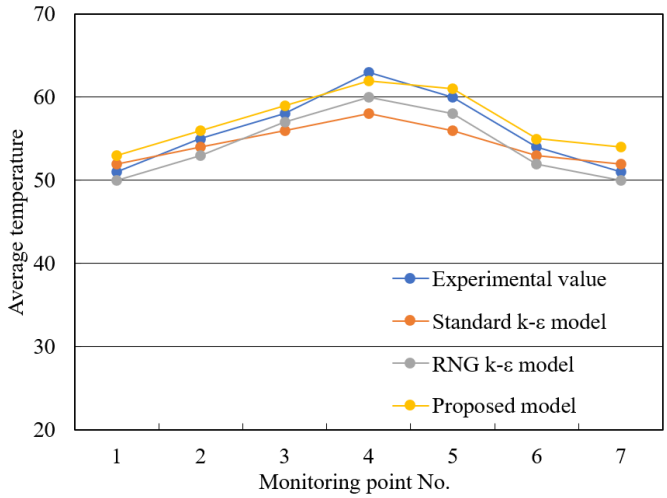

Figure 8. Comparison of different models in computational accuracy

Table 1. Variation pattern of the average equipment space temperature under different component spacing in the confined space

Spacing/*mm*	**2**	**3**	**4**	**5**	**6**	**7**	**8**
Heating power/*W*	50	50	50	50	50	50	50
Average space temperature/*K*	415.2	425.6	413.1	423.8	418.4	429.6	426.4
Ambient temperature/*K*	302.24	301.57	306.48	302.75	301.95	306.25	302.17
Spacing /*mm*	**9**	**10**	**11**	**12**	**13**	**14**	
Heating power/*W*	50	50	50	50	50	50	
Average space temperature/*K*	413.8	435.2	426.8	417.4	432.6	415.7	
Ambient temperature/*K*	303.68	303.48	302.49	301.64	302.48	305.27	

Table 2. Relationship between the heat transfer temperature difference and the height of the confined space

Height of the confined space/*mm*	**11**	**16**	**22**	**26**	**31**
Heat transfer temperature difference/*K*	122.24	98.57	93.26	90.14	89.58
Ambient temperature /*K*	302.15	301.48	303.29	302.81	301.74
Heating power /*W*	50	50	50	50	50
Height of the confined space/*mm*	**36**	**42**	**48**	**52**	**57**
Heat transfer temperature difference/*K*	92.48	92.63	93.68	94.15	95.26
Ambient temperature /*K*	305.85	303.62	301.74	304.59	302.16
Heating power /*W*	50	50	50	50	50

Table 3. Monitoring data of different components of the equipment when the ambient temperature is fixed

Component		Working condition 1	Working condition 2	Working condition 3	Working condition 4	Mean
	1	50.15	51.36	52.14	53.62	
	2	52.48	53.26	53.75	55.27	
A	3	53.62	54.18	54.71	55.62	53.682
	4	52.64	53.74	50.27	52.29	
	5	51.47	52.62	50.16	53.68	
	1	52.62	50.48	52.13	50.64	
	2	52.42	55.62	56.84	54.18	
B	3	53.26	57.49	58.26	55.15	55.817
	4	50.24	53.62	55.79	53.61	
	5	53.64	50.14	51.72	52.37	
	1	54.16	54.28	52.37	55.61	
	2	55.49	57.84	58.49	53.26	
C	3	55.17	52.24	54.72	51.27	56.748
	4	55.86	52.64	50.62	56.57	
	5	55.14	57.42	55.26	57.49	
	1	54.17	57.49	56.24	51.26	
	2	53.16	57.49	53.26	53.16	
D	3	53.28	54.11	50.75	51.49	53.264
	4	53.86	55.62	57.49	52.18	
	5	52.16	57.19	52.62	51.37	

Table 4. Average temperatures of the temperature monitoring positions under different models

Temperature monitoring position	Experimental value	Standard k-ε model	*RNG* k-ε model	Proposed model
1	50.267	55.162	51.248	50.192
2	61.361	57.492	55.263	61.274
3	63.495	62.482	56.418	62.185
4	62.174	63.295	58.492	63.152
5	58.728	59.514	55.628	59.472
6	61.112	61.689	57.146	61.241
7	59.228	54.136	52.856	59.287

6. CONCLUSION

This paper conducted numerical analysis and optimization of the space heat dissipation of mechanical automation equipment based on a thermal model. Firstly, the heat dissipation mechanism of mechanical automation equipment was elaborated in detail, and the structure of the heat dissipation system of mechanical automation equipment was presented. Then, the spatial thermal model of mechanical automation equipment was established, and the heat dissipation design process of mechanical automation equipment was given. Finally, the difference between natural convection heat dissipation in large space and that in the confined space inside the mechanical automation equipment was explored. Through experiments, the variation pattern of the average temperature of equipment space and the relationship between the heat transfer temperature difference and the height of the confined space with different component spacing were explored. Through summary of the monitoring data of different components of the equipment and the average temperatures at the temperature monitoring positions under different models, the calculation accuracy of different models was compared, which showed the effectiveness of the proposed numerical simulation model.

REFERENCES

[1] Cheng, H.P., Tsai, S.M., Cheng, C.C. (2014). Analysis of heat transfer mechanism for shelf vacuum freeze-drying equipment. Advances in Materials Science and Engineering, 2014: 515180. https://doi.org/10.1155/2014/515180

[2] Davidenko, N.N., Berezanin, A.A., Usanov, A.I. (2009). Application of diagnostic systems for monitoring the state of heat-transfer and mechanical equipment at nuclear power stations. Thermal engineering, 56(5): 363-369. https://doi.org/10.1134/S0040601509050024

[3] Alipourtarzanagh, E., Chinnici, A., Nathan, G.J., Dally, B.B. (2020). Experimental insights into the mechanism of heat losses from a cylindrical solar cavity receiver equipped with an air curtain. Solar Energy, 201: 314-322. https://doi.org/10.1016/j.solener.2020.03.004

[4] Bakirov, M.B., Kamyshnikov, O.G., Potapov, V.V. (2007). Managing the service life of heat-exchanging and mechanical equipment and pipelines operating at Russian nuclear power stations. Thermal engineering, 54(2): 87-93. https://doi.org/10.1134/S0040601507020012

[5] Qiu, T.Q., Xiang, Y., Lu, H.Q., Xie, C.F. (2006). Mechanism of scale controlling of heat-transfer equipment by ultrasonic. Huanan Ligong Daxue Xuebao (Natural Science), 34(3): 23-28.

[6] Alabugin, A.A., Alyukov, S.V., Osintsev, K.V. (2020). Approximation methods for analysis and formation of mechanisms for regulating heat and mass transfer processes in heat equipment systems. International Journal of Heat and Technology, 38(1): 45-58. https://doi.org/10.18280/ijht.380106

[7] Jorge, J.C.F., Faragasso, S.M., Guimarães de Souza, L.F., de Souza Bott, I. (2015). Effect of post-welding heat treatment on the mechanical and microstructural properties of extra high-strength steel weld metals, for

application on mooring equipment. Welding International, 29(7): 521-529. https://doi.org/10.1080/09507116.2014.932984

[8] Tarasenko, Y.P., Tsareva, I. N., Berdnik, O.B., Fel, Y.A., Kuzmin, V.I., Mikhalchenko, A.A., Kartaev, E.V. (2014). The structure and physical-mechanical properties of the heat-resistant Ni-Co-Cr-Al-Y intermetallic coating obtained using rebuilt plasma equipment. Thermophysics and Aeromechanics, 21(5): 641-650. https://doi.org/10.1134/S0869864314050138

[9] Golter, P., Van Wie, B., Coon, L. (2017). Capabilities of Desktop Scale Heat Transfer and Fluid Mechanics Equipment for Classroom Instruction. International Journal of Engineering Education, 33(4): 1163-1179.

[10] Grin, E.A. (2013). The possibilities of fracture mechanics as applied to problems of strength, service life, and substantiation of safe operation of heat-generating and mechanical equipment. Thermal Engineering, 60(1): 24-31. https://doi.org/10.1134/S0040601513010011

[11] Rezinskikh, V.F., Grin, E.A. (2013). Modern problems concerned with ensuring safe operation of heat-generating and mechanical equipment in extending its lifetime. Thermal Engineering, 60(1): 16-23. https://doi.org/10.1134/S0040601513010072

[12] Qu, J., Zhang, J., Li, M., Tao, W. (2020). Heat dissipation of electronic components by ionic wind from multi-needle electrodes discharge: Experimental and multi-physical analysis. International Journal of Heat and Mass Transfer, 163: 120406. https://doi.org/10.1016/j.ijheatmasstransfer.2020.120406

[13] Huang, D.S., Tu, W.B., Zhang, X.M., Tsai, L.T., Wu, T.Y., Lin, M.T. (2016). Using Taguchi method to obtain the optimal design of heat dissipation mechanism for electronic component packaging. Microelectronics Reliability, 65: 131-141. https://doi.org/10.1016/j.microrel.2016.07.006

[14] Abu-Nada, E., Pop, I., Mahian, O. (2019). A dissipative particle dynamics two-component nanofluid heat transfer model: application to natural convection. International Journal of Heat and Mass Transfer, 133: 1086-1098. https://doi.org/10.1016/j.ijheatmasstransfer.2018.12.151

[15] Wang, Y., Wei, B. (2014). Wet multi-disc friction components heat dissipation capability and optimal oil supply under continuous braking condition. Industrial Lubrication and Tribology, 66(6): 653-661. https://doi.org/10.1108/ILT-06-2012-0060

[16] Cavalcanti, E.J., Carvalho, M. (2021). Tackling dissipative components based on the SPECO approach: A cryogenic heat exchanger used in natural gas liquefaction. Energies, 14(20): 6850. https://doi.org/10.3390/en14206850

[17] Mohaupt, M., Van Oost, S., Barremaecker, L. (2019). The two-phase spreading of high heat fluxes density dissipative components for space and non-space applications. Heat Transfer Engineering, 40(3-4): 247-257. https://doi.org/10.1080/01457632.2018.1426250

[18] Riaz, A., Basit, A., Ibrahim, A., Shah, A., Basit, M.A. (2018). A three-dimensional CFD and experimental study to optimize naturally air-cooled electronic equipment enclosure: Effects of inlet height, heat source position, and buoyancy on mean rise in temperature. Asia‐Pacific Journal of Chemical Engineering, 13(1): e2145. https://doi.org/10.1002/apj.2145

[19] Wang, L., Li, L. M., Zeng, G.Q., Sun, J.L., Wu, L., Wang, H., Dai, Y.X. (2017). Thermal sturcutre design of air-cooled heat sinks for power electronic equipments by constrained population extremal optimization. In 2017 Chinese Automation Congress (CAC), Jinan, China, pp. 2467-2472. https://doi.org/10.1109/CAC.2017.8243190

[20] Satake, A., Jike, J., Mitani, Y. (2020). Consideration of peak cut method by air conditioning equipment corresponding to demand for contract power reduction-application of thermal radiative cooling/heating system. Energy Reports, 6: 768-774. https://doi.org/10.1016/j.egyr.2020.11.132

[21] Li, H., Ni, L., Yao, Y., Sun, C. (2019). Experimental investigation on the cooling performance of an Earth to Air Heat Exchanger (EAHE) equipped with an irrigation system to adjust soil moisture. Energy and Buildings, 196: 280-292. https://doi.org/10.1016/j.enbuild.2019.05.007

[22] Karami, A., Rezaei, E., Rahimi, M., Zanjani, M. (2012). Artificial neural modeling of the heat transfer in an air cooled heat exchanger equipped with butterfly inserts. International Energy Journal, 13(1): 21-28.

[23] Kuntysh, V.B., Sukhotskii, A.B., Piir, A.E. (2012). Effect of height of helical fin on convective heat transfer and energy and volume characteristics of heat-exchange sections in air-cooling equipment. Chemical and Petroleum Engineering, 48(7): 469-477. https://doi.org/10.1007/s10556-012-9641-0